

OPTIMIZING MOMENTUM APERTURE IN KOREA-4GSR VIA HIGHER-ORDER CHROMATICITY AND W-FUNCTION ANALYSES

Junha Kim^{*,1,2}, Jaehyun Kim^{†,2}, Gyeongsu Jang², Jimin Seok²,
Jaeyu Lee², Hyunchang Jin⁴, Moses Chung^{‡,3}

¹Ulsan National Institute of Science and Technology (UNIST), Ulsan, Republic of Korea

²Pohang University of Science and Technology, Pohang, Gyeongbuk, Republic of Korea

³Pohang Accelerator Laboratory, POSTECH, Pohang, Gyeongbuk, Republic of Korea

⁴Korea Basic Science Institute, Cheongju, Korea

Abstract

Diffraction-limited light sources require strong magnets that inevitably induce severe nonlinear effects and limit the Touschek lifetime (TLT). In this study, systematic tune and chromaticity scans were performed for the Korea-4GSR to identify optimal working points and characterize lattice properties under realistic errors. Analyzing momentum-dependent tune shift (MDTS) profiles clarified the physical mechanism behind the error-induced chromaticity preference. Because direct tracking-based lifetime optimization is computationally prohibitive, we propose an efficient indirect optimization method that targets the minimization of chromatic W -function fluctuations, effectively bypassing the multi-turn tracking bottleneck.

INTRODUCTION

The Korea-4GSR storage ring utilizes 28 Hybrid 7-Bent Achromat (H7BA) cells to achieve an ultralow emittance, incorporating 26 insertion device straight sections and 2 high- β sections [1]. Although the ring possesses a 2-fold geometric symmetry, it maintains a 28-cell symmetry in terms of on-momentum phase advances [2]. However, the extremely strong quadrupoles and sextupoles required for emittance reduction induce severe nonlinear beam dynamics, restricting the momentum aperture (MA) and limiting the TLT.

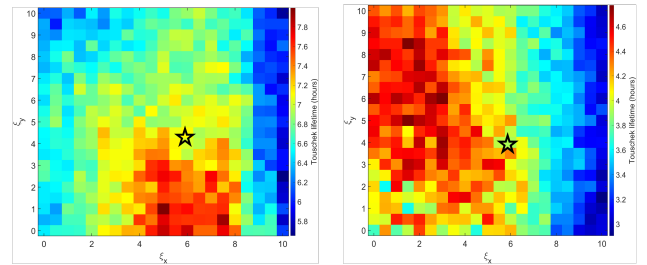
To identify the optimal operating working points for maximizing the TLT baseline, systematic chromaticity scans were executed under both ideal and error-affected conditions, revealing a distinct discrepancy in lifetime behavior depending on lattice errors. To navigate this error-induced regime, a direct tracking-based Multi-Objective Genetic Algorithm (MOGA) optimization was first performed to maximize on-momentum dynamic aperture (DA) and tracking-derived TLT.

The optimization results closely matched the scans, and deeper analysis highlighted correlation between suppressed off-momentum chromatic W -function fluctuations and enhanced TLT baseline. Guided by this physical relation, an indirect MOGA optimization framework was formulated. Replacing the intensive multi-turn tracking loops with the

fast minimization of W -function fluctuations eliminated the computational bottleneck, drastically accelerating the optimization speed while securing a robust lattice design.

SYSTEMATIC LATTICE SCANS

Systematic 2D chromaticity scans (ξ_x, ξ_y) were performed to explore off-momentum dynamics. As shown in Fig. 1, a striking discrepancy in TLT behavior is observed between the lattices. In the ideal bare lattice (Fig. 1a), the peak lifetime occurs at higher horizontal (ξ_x) and lower vertical chromaticity (ξ_y). Conversely, introducing realistic errors shifts this preference to a low ξ_x and high ξ_y region (Fig. 1b). This occurs because off-momentum particles easily survive integer resonance crossings in the bare lattice where driving terms are weak, whereas errors severely amplify these resonances, triggering premature beam loss as soon as the tunes hit the integer lines.



(a) Bare lattice

(b) Error lattice

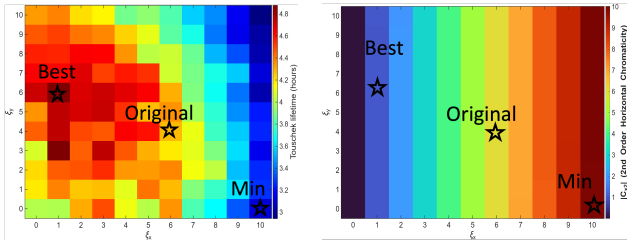
Figure 1: Systematic chromaticity scans (ξ_x, ξ_y) evaluating the Touschek lifetime for (a) the ideal bare lattice and (b) the error lattice with alignment and multipole errors. The color bars indicate the Touschek lifetime in hours. The black stars represent the initial chromaticity configuration.

To clarify this mechanism, the second-order horizontal chromaticity $|C_{x,2}|$ was mapped, revealing a strong inverse correlation with the TLT distribution (Fig. 2). Insufficient lifetime configurations (Min) correspond precisely to regions where $|C_{x,2}|$ is excessively amplified, whereas the optimal configuration (Best: $\xi_x = 1, \xi_y = 6$) minimizes this term. This relationship is confirmed by the MDTS curves evaluated in the dispersion-free region (Fig. 3). Minimizing $|C_{x,2}|$ flattens and broadens the parabolic tune footprint, delaying off-momentum particles from intersecting the destructive integer resonance line ($\nu_x = 69.0$), thereby extending the MA and lifetime.

* joonha9609@postech.ac.kr

† Corresponding author: picoma@postech.ac.kr

‡ Corresponding author: mooses@postech.ac.kr



(a) Tauschek lifetime map (b) 2nd-order horizontal chromaticity

Figure 2: Systematic chromaticity scans (ξ_x, ξ_y) mapping (a) the Tauschek lifetime under error lattice and (b) the absolute value of the second-order horizontal chromaticity $|C_{x,2}|$. The stars indicate the initial (Original), optimal (Best), and minimum performance (Min) operating configurations.

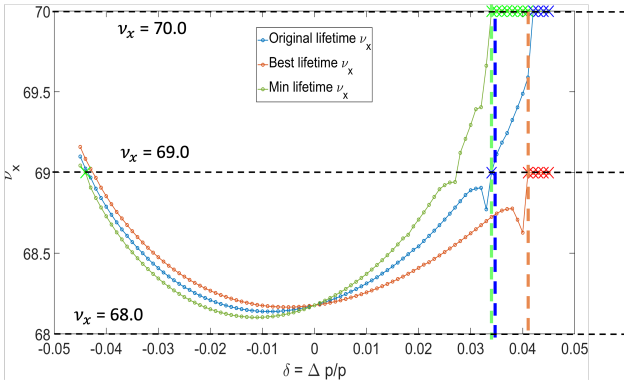
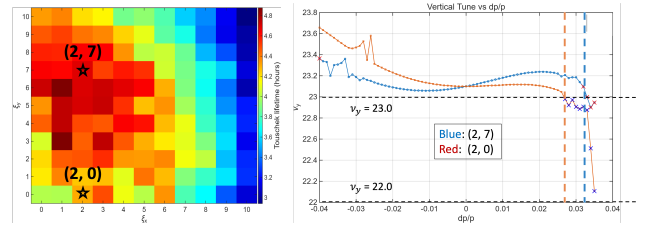


Figure 3: Momentum-dependent tune shift (MDTS) curves in the dispersion-free region under different chromaticity configurations (Original, Best, and Min).

To evaluate the vertical chromaticity impact, the horizontal chromaticity was fixed at $\xi_x = 2$ to compare configurations at $(\xi_x, \xi_y) = (2, 7)$ and $(2, 0)$, as shown in Fig. 4. Unlike the dispersion-free section, the MDTS behavior at the dispersion bump is dominated by the third-order chromaticity. As shown by the vertical MDTS profiles (Fig. 4b), increasing the vertical chromaticity to $\xi_y = 7$ (blue curve) steepens the tune shift near the on-momentum ($\delta = 0$) point. This steepness shifts the overall footprint, delaying the destructive crossing of the integer resonance line ($\nu_y = 23.0$) to a larger momentum deviation, which widens the vertical MA and secures the higher vertical chromaticity preference.

DIRECT TRACKING-BASED MOGA OPTIMIZATION

A Multi-Objective Genetic Algorithm (MOGA) framework via the pymoo [3] library was implemented to simultaneously maximize both the on-momentum DA area and the TLT under realistic error conditions, with all lattice simulations and tracking loops evaluated using Accelerator Toolbox (AT) [4, 5]. Figure 5(a) illustrates the evolutionary progress of the Pareto front in the objective space over 120 generations, showing a steady advancement toward the upper-right region. From the final population, Solution A (indicated by

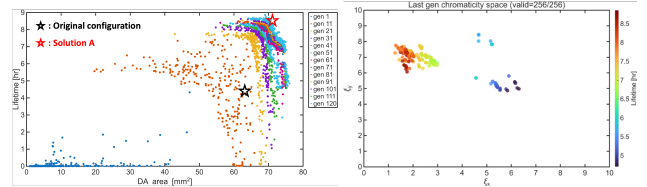


(a) Tauschek lifetime map (b) Vertical MDTS curve

Figure 4: Systematic chromaticity scans (ξ_x, ξ_y) evaluating (a) the Tauschek lifetime with error and (b) MDTS curves for the vertical tune ν_y at the dispersion bump. The stars in (a) indicate the benchmark configurations at $(\xi_x, \xi_y) = (2, 7)$ and $(2, 0)$, which correspond to the blue and red curves in (b), respectively.

the red star) was selected to achieve the best compromise between DA and lifetime.

The parameter convergence of the optimized lattices is evaluated by mapping the distribution of the last generation within the chromaticity space (ξ_x, ξ_y), as shown in Fig. 5(b). The final population cleanly clusters within the low horizontal and high vertical chromaticity regime, demonstrating excellent agreement with the optimal operating region identified during the systematic error-lattice scans.



(a) Objective space evolution (b) Last generation distribution

Figure 5: MOGA optimization results showing (a) the optimization progress in the objective space, where the red star represents the selected optimal solution, and (b) the lifetime of the last generation plotted within the chromaticity space.

The nonlinearity of Solution A was evaluated by comparing the chromatic W-functions (W_x, W_y) along the ring with those of the original lattice, as shown in Fig. 6. Under large off-momentum deviations, the optimized configuration (red line) exhibits significantly smaller fluctuations and more stable behavior across the entire ring. This suppression is particularly pronounced at $\delta = +3.0\%$, where the peak-to-peak amplitude of the W-function is drastically reduced. This strong correlation between suppressed W-function fluctuations and enhanced TLT indicates that local chromatic beta-beating plays a critical role in limiting off-momentum dynamics. A secondary optimization strategy can therefore be established to indirectly maximize the lifetime by explicitly minimizing the W-function fluctuations along the ring.

INDIRECT OPTIMIZATION

An indirect MOGA framework was established starting from the bare area lattice to accelerate the optimization speed.

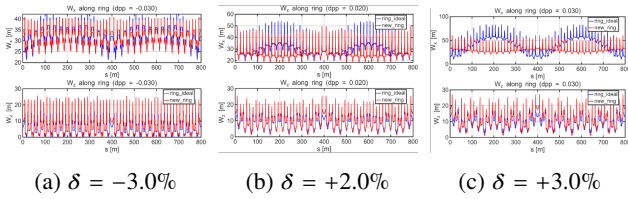


Figure 6: Comparison of chromatic W -functions (W_x, W_y) along the storage ring between the original configuration (ring_ideal, blue) and the optimized Solution A (new_ring, red) evaluated at momentum deviations of (a) $\delta = -3.0\%$, (b) $\delta = +2.0\%$, and (c) $\delta = +3.0\%$.

This approach replaces heavy tracking-based lifetime evaluations with two fast, physics-motivated objectives: the RMS-type measures of off-momentum chromatic W -function fluctuations along the ring, evaluated specifically at $\pm 4.0\%$ to target the momentum aperture (MA) boundary of the original machine, and an on-momentum resonance driving term (RDT) metric to preserve the DA [6, 7]. Bypassing tracking simulations significantly reduced the computation time per generation from approximately 4 hours to just 5 minutes. This computational efficiency enabled an expanded optimization scale, utilizing a population size of 1024 across 200 generations with 12 tuning variables (sextupole and octupole strengths). Constraints from prior scans were also enforced to steer the algorithm toward the favorable chromaticity regime.

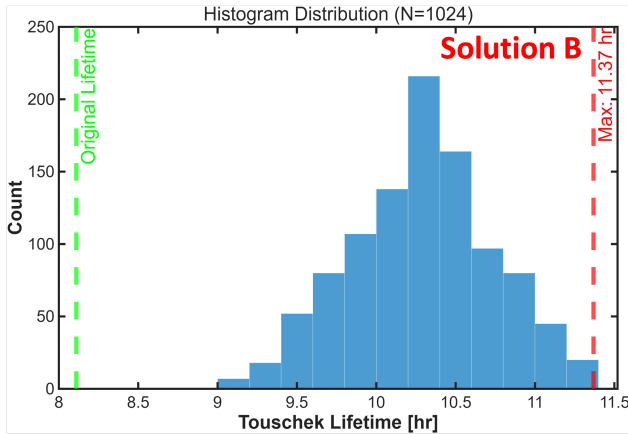


Figure 7: Histogram distribution of the Touschek lifetime ($N = 1024$) obtained from the indirect optimization targeting W -function minimization. The green dashed line marks the original baseline, while the red dashed line denotes the maximum achieved lifetime candidate, designated as Solution B.

The final-generation population yields a significantly improved TLT distribution compared to the original configuration, as shown in Fig. 7. In the ideal no-error case, every candidate demonstrates an extended lifetime, with the peak performer (Solution B) reaching 11.37 hours. Statistical validation using random lattice error ensembles confirms the robustness of this solution, as illustrated in Fig. 8. Under the reduced-error ensemble, Solution B achieves a 57.6% increase in average TLT. Importantly, this lifetime gain re-

mains highly consistent against both the reduced-error and full correction-chain ensembles, proving the practical reliability of the indirect optimization approach.

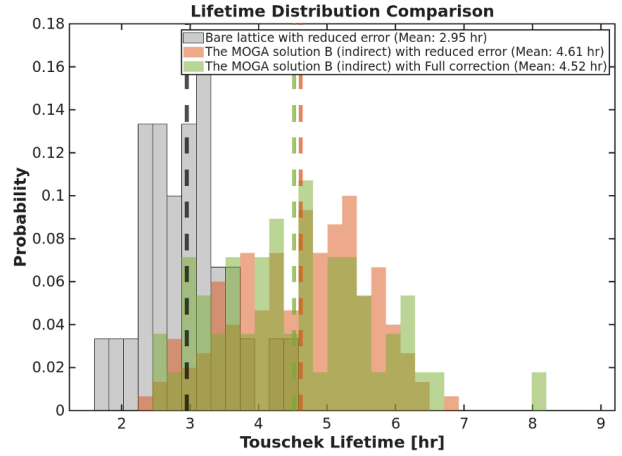


Figure 8: Touschek lifetime distribution comparison evaluated under random lattice error ensembles. The plots contrast the performance of the bare lattice against the MOGA-derived Solution B under both reduced error and full correction schemes.

CONCLUSION

Systematic beam dynamics investigations and optimization frameworks were successfully implemented to address the nonlinear limitations of the Korea-4GSR storage ring. Chromaticity and MDTs scans revealed that lattice errors severely amplify driven resonance lines, triggering premature off-momentum beam loss, whereas suppressing the tune footprint curvature successfully delays these destructive crossings.

While direct tracking-based MOGA verified these scans, it exposed a strong correlation between reduced off-momentum chromatic W -function fluctuations and enhanced Touschek lifetimes. Inspired by this, a fast, indirect MOGA framework was formulated using W -function RMS fluctuations and on-momentum RDTs as objectives.

Bypassing tracking loops significantly reduced the computation time per generation from 4 hours to 5 minutes, enabling an expanded optimization with a population of 1024 over 200 generations. This indirect approach yielded Solution B, achieving an ideal peak lifetime of 11.37 hours. Random error ensemble simulations statistically validated that Solution B delivers a 57.6% increase in average Touschek lifetime with high stability across various correction schemes, confirming the practical efficiency and reliability of the proposed indirect strategy.

REFERENCES

[1] G. Jang *et al.*, “Low emittance lattice design for Korea-4GSR”, *Nucl. Instrum. Methods Phys. Res. A*, vol. 1034, p. 166799, 2022. doi:10.1016/j.nima.2022.166779

- [2] J. Kim, G. Jang, J. Lee, and J. Seok, “The Korea-4GSR storage ring lattice design”, in *Proc. IPAC’25*, Taipei, Taiwan, Jun. 2025, pp. 789–792. doi:10.18429/JACoW-IPAC2025-MOPS089
- [3] J. Blank and K. Deb, “Pymoo: multi-objective optimization in Python”, *IEEE Access*, vol. 8, pp. 89497–89509, 2020. doi:10.1109/ACCESS.2020.2990567
- [4] A. Terebilo, “Accelerator Toolbox for MATLAB”, SLAC National Accelerator Laboratory, Menlo Park, CA, USA, Rep. SLAC-PUB-8732, 2001.
- [5] Accelerator Toolbox Collaboration, <https://github.com/atcollab/at>
- [6] J. Kim *et al.*, “Optimization of the Korea-4GSR storage ring for increasing the off-momentum dynamic aperture by analyzing resonance driving terms”, in *Proc. IPAC’25*, Taipei, Taiwan, Jun. 2025, pp. 887–890. doi:10.18429/JACoW-IPAC2025-TUBD3
- [7] B. Wei, Z. Bai, J. Tan, L. Wang, and G. Feng, “Minimizing the fluctuation of resonance driving terms in dynamic aperture optimization”, *Phys. Rev. Accel. Beams*, vol. 26, p. 084001, 2023. doi:10.1103/PhysRevAccelBeams.26.084001